

Thermoluminescence: theory

Fabrice Rappaport · Jérôme Lavergne

Received: 23 December 2008 / Accepted: 14 May 2009 / Published online: 17 June 2009
© Springer Science+Business Media B.V. 2009

Abstract Thermoluminescence (TL) probes the emission of luminescence associated with the de-trapping of a radical pair as the temperature is increased. This technique has proved useful for characterizing the energetic arrangement of cofactors in photosynthetic reaction centers. In the original TL theory, stemming from solid-state physics, the radical pair recombination was considered to coincide with the light-emitting process. In photosynthetic systems, however, recombination takes place through various routes among which the radiative pathway generally represents a relatively minor leak, and the theoretical framework must be modified accordingly. The radiative route is the one with the largest activation energy and is thus (still) more disfavored at low temperature, so that during the heating process, the TL peak tends to lag behind the decay of the radical pair. A consequence is that the integrated luminescence emission increases with the heating rate. In this article, we examine how the characteristics of the TL emission depend on the redox potentials of the cofactors, showing good agreement between theory and experimental studies on Photosystem (PS) II mutants. We also analyze

the effect on (thermo-) luminescence of the connectivity of the light-harvesting pigment antenna, and show that while this should affect significantly luminescence kinetics at room temperature, the effect on TL is expected to be small.

Keywords Photosynthesis · Electron transfer · Energetic · Luminescence · Photosystem II

Abbreviations

PS II Photosystem II
RC Reaction center
TL Thermoluminescence

Introduction

The term luminescence covers various processes of “cold” light emission. In photosynthesis, it refers to the reverse process of charge separation, involving the thermal formation of the singlet excited state of the primary photochemical electron donor from some charge-separated state (“radical pair”) of lower energy. Thermodynamics tells us that such a process must exist (because of microscopic reversibility), but says nothing about its yield. The decay of the radical pair is a very exergonic process and one expects that it may occur through routes that spare the thermal kick required for exciting a chlorophyll. Depending on the relative importance of the radiative/non-radiative processes, Lavorel (1975) distinguished “deactivation-type luminescence”, where non-radiative recombination is negligible, and “leakage-type luminescence”, where light emission does not interfere significantly with the decay process—but allows us to monitor it. It has turned out that photosynthetic luminescence is, in fact, rather of the leakage type and this

F. Rappaport (✉)
Institut de Biologie Physico-Chimique, Unité Mixte de
Recherche 7141 CNRS (Centre National de la Recherche
Scientifique), Université Paris 6, 13 Rue Pierre et Marie Curie,
75005 Paris, France
e-mail: Fabrice.Rappaport@ibpc.fr

J. Lavergne
Laboratoire de Bioénergétique Cellulaire Unité Mixte de
Recherche 6191 CNRS (Centre National de la Recherche
Scientifique), CEA (Commissariat à l’Energie Atomique)-
Université Aix Marseille II- CEA Cadarache,
13108 Saint Paul-lez-Durance, France
e-mail: Jerome.Lavergne@cea.fr

implies significant readjustments of the theory that had been used for analyzing thermoluminescence (TL) data.¹

Thermoluminescence is luminescence monitored from the pre-illuminated sample when it is heated at a constant rate: it provides information on the depth of the energy stabilization of the charge-separated state(s) initially present and on their amount. Apart from its use in photosynthesis, TL is a popular technique for monitoring the age of the samples (see, for example, Miallier et al. 2006). Some substances such as quartz or fluorite store energy when exposed to radiation and this trapped energy can be released while emitting light when heating the sample. The integrated light emission allows the determination of the age of the sample (i.e., dating) under the assumption that the amount of trapped radical pairs has steadily increased throughout time.

Luminescence

Figure 1 depicts the simplest situation, involving three states: the ground state S_g , the excited singlet S^* and the metastable state S_e whose free energy level is located at ΔG_{exc} below that of S^* (we are dealing here with molecular, standard free energy levels, usually written with subscript 0, omitted here for simplicity; our sign convention is that ΔG_{exc} is positive when S_e lies at a lower energy than S^*). This is a shorthand notation for states that we might otherwise denote as PA, P*A, and P⁺A⁻, respectively, where P is the photochemical electron donor and A an electron acceptor. The rate constant for the decay of S^* to S_g is k_{rad} . This process is accompanied by the emission of a photon with a probability Φ (the alternative is heat emission with probability $1 - \Phi$). The charge separation takes place with rate constant k_1 . The rate constant for the backward process is k_{-1} , related to k_1 and ΔG_{exc} by

$$\frac{k_{-1}}{k_1} = e^{-\frac{\Delta G_{\text{exc}}}{k_B T}}, \quad (1)$$

where k_B is Boltzmann's constant.

The direct, non-radiative decay of S_e to S_g (e.g., the electron tunneling from A⁻ to P⁺) is shown as a dashed line, with rate constant k_{nr} . For the time being, we do not need to specify whether this route is negligible or not. Denoting as $n(t)$ the

¹ In his 1975 article, Jean Lavorel believed that “leakage-type” luminescence should predominate at short times after a flash (during the stabilization steps of the radical pair), while it could become “deactivation type” at longer times when electron transfer equilibrium is achieved on the donor and acceptor sides. He did not consider the possibility of *non-radiative recombination*, which is in fact a major pathway, as explained later. Nevertheless, the distinction between luminescence as a “passive” monitoring of the decay (leakage type) or as the very cause of the decay (deactivation type) remains relevant.

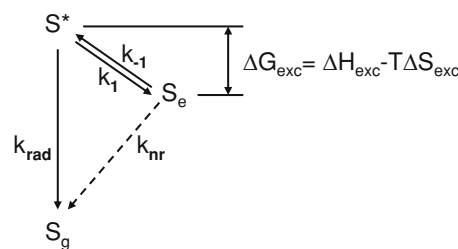


Fig. 1 A basic scheme for charge separation and recombination. The metastable state S_e can decay either through the radiative route involving a thermal jump to S^* and the decay of S^* to S_g (with a probability Φ to emit a photon) or through the non-radiative route indicated by the dashed arrow. “Deactivation-type” luminescence corresponds to the case where the non-radiative route is negligible (as assumed in the Randall–Wilkins treatment of TL), whereas “leakage-type” luminescence corresponds to the case where the non-radiative route is predominant

fraction of our system in state S_e at time t , the rate of the decay through the luminescence pathway can be written as

$$L(t) = \Phi k_{\text{exc}} n(t). \quad (2)$$

The effective rate constant k_{exc} featuring in Eq. 2 is

$$k_{\text{exc}} = k_{-1} \frac{k_{\text{rad}}}{k_{\text{rad}} + k_1}. \quad (3)$$

The above equations rely on a so-called steady-state approximation, which is valid after the initial relaxation between S^* and S_e has occurred (i.e., at times longer than $1/k_1$). We also assume that the equilibrium constant between S^* and S_e is largely in favor of the latter ($k_1 \gg k_{-1}$). In Eq. 3, the fraction on the right-hand side expresses the probability that any newly formed S^* state decays to S_g rather than (back) to S^* . Two extreme cases may be considered. If $k_1 \gg k_{\text{rad}}$, one has

$$k_{\text{exc}} = k_{-1} \frac{k_{\text{rad}}}{k_1} = k_{\text{rad}} e^{-\frac{\Delta G_{\text{exc}}}{k_B T}} = k_{\text{rad}} e^{-\frac{\Delta S_{\text{exc}}}{k_B} - \frac{\Delta H_{\text{exc}}}{k_B T}}. \quad (4)$$

The latter expression uses the decomposition of ΔG_{exc} into an enthalpy term, ΔH_{exc} and an entropic term $-T\Delta S_{\text{exc}}$. In this picture, the excited state is in rapid equilibrium with S_e and plays the role of the “activated” or “transition” state of Arrhenius or Eyring rate theories. In the opposite case where $k_1 \ll k_{\text{rad}}$, one has simply $k_{\text{exc}} \approx k_{-1}$, reflecting the fact that the whole process is rate limited by the uphill jump from S_e to S^* . In this case, the temperature dependence of k_{exc} (i.e., of k_{-1}) may involve an activation energy larger than ΔH_{exc} , if the forward process from S^* to S_e is not activationless. However, primary charge separation reactions are generally activationless, so that we can disregard this possibility and express k_{exc} in a general form

$$k_{\text{exc}} = s \exp\left(-\frac{\Delta H_{\text{exc}}}{k_B T}\right). \quad (5)$$

The pre-exponential factor s ($k_{\text{rad}} e^{\frac{\Delta G_{\text{exc}}}{k_B}}$ if Eq. 4 is valid or an equivalent expression for k_{-1} in the opposite case) is temperature independent. Our reason for discussing these cases and showing that Eq. 5 is of general validity is that PS II appears to be midway between the two cases discussed above, with $k_{\text{rad}} \sim k_1$ (Van Gorkom 1985; Rappaport et al. 2002; Cuni et al. 2004).

We have adopted here an Arrhenius’ rather than Eyring’s rate theory (see Vass et al. 1981, for the latter approach), since the latter would involve a temperature-dependent contribution in the pre-exponential factor, namely $k_B T/h$ (h is Planck’s constant). Our only reason for doing so is that consideration of the Eyring term is of little quantitative consequence (because its temperature dependence is much less steep than that of the exponential term) so that the simpler formulation can be retained without any significant consequence.

The luminescence intensity at a given time, t , and temperature, T , is (using Eqs. 2 and 5)

$$L(t, T) = \Phi k_{\text{exc}}(T) n(t, T) = \Phi s \exp\left(-\frac{\Delta H_{\text{exc}}}{k_B T}\right) n(t, T). \tag{6}$$

This expression shows that luminescence can be used as a kinetic means of monitoring the amount of some state S_e as a function of time (e.g., following a flash) or, focusing on the exponential term, as information on the energetic landscape (how large is ΔH_{exc}). Such an approach has been followed by numerous authors to characterize the energetics of reaction centers (see, for example, Joliot et al. 1971; Borisov et al. 1980; Booth et al. 1991; Peloquin et al. 1994; Grabolle and Dau 2005).

Thermoluminescence: the Randall–Wilkins scheme

An obvious consequence of Eq. 6 is that luminescence will be very weak when ΔG_{exc} is large with respect to $k_B T$ (25 meV at 25°C), so that one is tempted to heat the sample to improve the sensitivity. This is probably one of the reasons for the success of TL in the study of photosynthesis (Arnold and Sherwood 1957; for reviews, see Inoue and Shibata 1979; Sane and Rutherford 1986; Vass and Govindjee 1996). This method consists in trapping S_e at low temperature (which may be done in various ways: for example, by illuminating the sample at room temperature and rapidly cooling it, or by cooling in the dark and illuminating at low T , or by cooling in the light) and monitoring the luminescence emission as the sample is slowly warmed up at a constant rate. The theoretical treatment of this problem, described below, was originally introduced in solid-state physics (Randall and Wilkins 1945).

The kinetic scheme considered by Randall and Wilkins (1945) is that of a “deactivation-type” luminescence, ignoring the possibility of alternative pathways (such as the dashed arrow in Fig. 1). Since the decay of S_e occurs through the sole radiative pathway, with rate constant k_{exc} , one has

$$\frac{dn(t)}{dt} = -k_{\text{exc}} n(t) = -\frac{L(t)}{\Phi}. \tag{7}$$

At constant temperature (constant k_{exc}), this would be readily integrated, giving $n(t) = n(0) \exp(-k_{\text{exc}} t)$. We ask: How about the TL situation where the temperature does change? The constant warming rate $B \equiv \frac{dT}{dt}$ provides a relation between the two variables determining the luminescence intensity $L(t, T)$. One may then rewrite Eq. 7 as

$$\frac{dn}{dT} = -\frac{k_{\text{exc}}}{B} n, \tag{8}$$

where k_{exc} depends on the temperature as expressed in Eq. 5. In order to integrate Eq. 8, one separates variables by moving n to the left-hand side and obtains

$$\ln \frac{n(T)}{n(T_0)} = -\frac{1}{B} \int_{T_0}^T k_{\text{exc}}(x) dx = -\frac{s}{B} \int_{T_0}^T e^{-\frac{\Delta H_{\text{exc}}}{k_B x}} dx. \tag{9}$$

Here, x is the variable temperature used as the integration variable. We have no analytical expression for the integral, but this does not matter; it is perfectly well defined and computable with any desired precision. The expression for n is then

$$n(T) = n(T_0) \exp\left(-\frac{s}{B} \int_{T_0}^T e^{-\frac{\Delta H_{\text{exc}}}{k_B x}} dx\right). \tag{10}$$

The starting temperature T_0 is generally chosen low enough so that the luminescence emission is negligible. One may make the convention $n(T_0) = 1$, as will be assumed henceforth.

Combining Eqs. 5, 7, and 10, one obtains

$$L(T) = \Phi s \exp\left[-\frac{\Delta H_{\text{exc}}}{k_B T} - \frac{s}{B} \int_{T_0}^T e^{-\frac{\Delta H_{\text{exc}}}{k_B x}} dx\right]. \tag{11}$$

This predicts that the TL emission has a dissymmetrical bell-shaped curve (for example, see Fig. 3A). The emission starts to rise when $k_B T$ ceases to be very small with respect to ΔH_{exc} ; it eventually declines because of the depletion of the metastable state S_e . The temperature T_m where the TL peak is observed is related to ΔH_{exc} . Indeed, when deriving Eq. 11 one finds that $\frac{dL}{dT} = 0$ implies that

$$\frac{\Delta H_{\text{exc}}}{k_B T^2} = \frac{s}{B} e^{-\frac{\Delta H_{\text{exc}}}{k_B T}}. \tag{12}$$

There is a unique value of $T = T_m$ which satisfies Eq. 12. Again, there is no analytical solution for this equation, but an accurate numerical solution is easily obtained.

Real photosynthetic reaction centers versus the simple Randall–Wilkins scheme

The model used in the preceding section leaves out some important features of the charge separation–recombination reactions in photosynthetic reaction centers (RC). First, many more states are involved, because of the successive stabilization steps on cofactors on the acceptor and donor sides. The temperature-dependent equilibrium between these states must be taken into account for a rigorous treatment. This was pointed out by Don DeVault and coworkers (DeVault et al. 1983; DeVault and Govindjee 1990) who refined the Randall–Wilkins treatment to incorporate such features. However, in the frequently encountered cases where the energy gap between the most stable charge-separated state and the other states is relatively large, the correction is negligible. As shown below, such is the case when dealing with the recombination of the $S_2Q_A^-$ state in PS II, but not, as pointed out by Rose et al. (2008) when studying the recombination of $S_2Q_B^-$. On the other hand, photosynthetic RCs diverge from the Randall–Wilkins scheme in a more important, qualitative manner (Rappaport et al. 2005). As indicated in the introduction, short circuit reactions (such as the dashed arrow in Fig. 1) constitute generally the main recombination pathway, and luminescence is of the “leakage” rather than “deactivation” type. Before examining how one should modify Eq. 10 to take this into account, we shall outline the reaction scheme for a definite type of reaction center, which has been the object of most TL studies: Photosystem II (PS II).

Figure 2 shows the various states of PS II that are relevant to the present discussion (see Rappaport and Diner 2008, for a recent review on PS II energetics). The donor chain includes, besides the electron donor P_{680} , a tyrosine (Y_Z) which reduces P^+ (oxidized P_{680}) in some tens of ns and is in turn reduced by an electron extracted from the Mn cluster of the water splitting enzyme (transition from S_1 to S_2) (Diner and Britt 2005; Hillier and Messinger 2005). On the acceptor side, the electron is transferred to the pheophytin (the primary electron acceptor) within a few picoseconds (see Barter et al. 2005; Renger and Holzwarth 2005 for reviews), then to the primary quinone acceptor Q_A within a few hundred picoseconds. The semiquinone Q_A^- is in turn re-oxidized by the secondary quinone Q_B . The latter electron transfer reaction can be blocked by inhibitors (e.g., DCMU, 3-(3,4-dichlorophenyl)-1,1-dimethylurea) which bind into the Q_B pocket. In the presence of such an inhibitor,

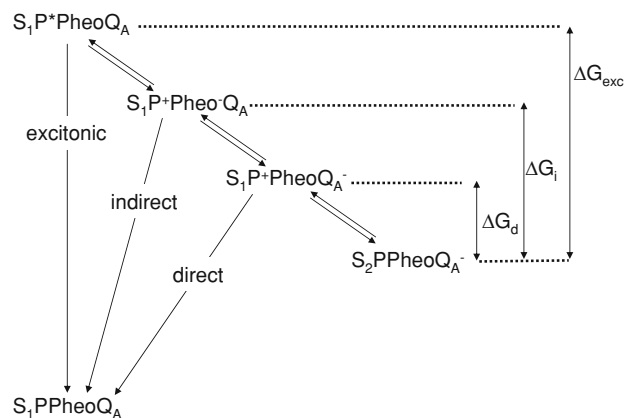


Fig. 2 Charge separation and recombination in PS II. The equilibrium between charge-separated states is overwhelmingly (99.99% at 300 K) in favor of the lowest energy state ($S_2Q_A^-$). Three recombination routes are indicated. The excitonic route (accompanied with the emission of a photon with probability Φ) accounts for $\sim 3\%$ of the overall decay at room T . The non-radiative routes are denoted as “direct” when the reduction of P^+ involves electron transfer from the semiquinone Q_A^- and “indirect” when the electron is transferred from Pheo $^-$. At room temperature, the indirect route accounts for about 77% of the overall decay and the direct route for about 20%. The still more direct route from Q_A^- to the Mn cluster (S_2) is negligible

the charge-separated state of lowest energy formed after a single turnover flash is thus $S_2Y_ZP_{680}PheoQ_A^-$ (noted as $S_2Q_A^-$ for brevity). At room temperature, the half-time for the recombination of this state (through mechanisms which are examined below) is about 2 s. In the absence of inhibitor, the lowest energy state is $S_2Q_B^-$, the recombination of which is about 20-fold slower than that of $S_2Q_A^-$.

In principle, even in the simpler case when the transfer to Q_B is blocked, there are many ways by which the final step of the recombination process (i.e., the transfer of the electron from the electron acceptor side to the electron donor side) could occur: the electron can reside on three possible carriers on the acceptor chain and the oxidized equivalent can also reside on three donors; thus, there are nine possibilities. Each of the nine candidate states can be formed through the electron transfer equilibria in each chain. It turns out that only three of these pathways occur at a significant rate (Rappaport et al. 2002; Cuni et al. 2004). All involve P^+ as the oxidation target, while the electron “donor” can be Q_A^- , Pheo $^-$, or P^* . In the last case, an excited chlorophyll is formed, which may decay with some probability of emitting a photon. This is the case where recombination occurs by the exact reverse of the photochemical process, giving rise to luminescence emission. We denote this as the excitonic or radiative (even though it is only partially so) pathway. Besides this, there are two non-radiative recombination routes. One is the “direct route” where Q_A^- is the electron donor. At variance with

the other ones, this route does not require the thermal population of the low potential acceptors; actually, the direct $P^+Q_A^- \rightarrow PQ_A$ reaction is activationless and occurs at cryogenic temperatures (see Rappaport et al. 2002, for a discussion). The second relevant recombination pathway is the “indirect route” where Pheo⁻ is the electron donor in state P^+Pheo^- (this state involves actually several sub-states, singlet and triplet, depending on the spin correlation between the two partners; see Van Gorkom 1985; Rappaport et al. 2002).

The relative yields of these three processes at room temperature are now fairly well known. It was shown by Van Gorkom and coworkers (De Grooth and Van Gorkom 1981; Van Gorkom 1985) that the yield of the excitonic pathway accounts for about 3% of the overall recombination. This implies that PS II luminescence is of the leakage, rather than deactivation, type. The yield of the indirect pathway has been estimated by comparing the lifetime of the $S_2Q_A^-$ state in PS II mutants in which the midpoint potential of the Pheo/Pheo⁻ couple, and hence the yield of the indirect pathway, was modified. The recombination rate of $S_2Q_A^-$ was found to depend quite significantly on the midpoint potential of pheophytin (the rate is faster when the potential gap between Ph and Q_A is diminished), demonstrating, as previously proposed by Van Gorkom (1985) and Vavilin and Vermaas (2000) that the excitonic pathway is efficiently by-passed by the indirect pathway (Cuni et al. 2004; Rappaport et al. 2005; Cser and Vass 2007). The comparison of the $S_2Q_A^-$ lifetime in the various mutants allowed a quantitative estimation of the rates and yields of the various pathways at room temperature. The yield of the direct pathway was found to be in the 15–20% range (Rappaport et al. 2002; Cser and Vass 2007) and that of the indirect route about 80–85% (including the ~3% yield of the excitonic pathway).

Photosynthetic TL theory (1): Implementation of non-radiative recombination

As argued above, the model used in the Randall–Wilkins treatment must be modified by considering that non-radiative recombination pathways are not necessarily negligible. When taking into account the dashed pathway in Fig. 1, with rate constant k_{nr} , one must modify Eq. 7 in the following way. The decay rate of S_e becomes

$$\frac{dn(t)}{dt} = -(k_{exc} + k_{nr})n(t), \tag{13}$$

while one still has

$$L(t) = \Phi k_{exc} n(t). \tag{14}$$

We denote as k_{tot} the sum $k_{exc} + k_{nr}$. The temperature

dependence of k_{nr} is assumed to have an Arrhenius’ form (like that of k_{exc} , Eq. 5)

$$k_{nr}(T) = s_{nr} \exp\left(-\frac{\Delta H_{nr}}{k_B T}\right). \tag{15}$$

Equation 13 is expressed as a function of T and integrated in the same way as above (see Eqs. 8–10), yielding

$$\begin{aligned} n(T) &= \exp\left(-\frac{1}{B} \int_{T_0}^T k_{tot}(x) dx\right) \\ &= \exp\left(-\frac{1}{B} \int_{T_0}^T \left(s_{exc} \exp\left(-\frac{\Delta H_{exc}}{k_B x}\right) + s_{nr} \exp\left(-\frac{\Delta H_{nr}}{k_B x}\right)\right) dx\right). \end{aligned} \tag{16}$$

The TL expression is (keeping the k_{tot} notation for brevity)

$$L(T) = \Phi s_{exc} \exp\left[-\frac{\Delta H_{exc}}{k_B T} - \frac{1}{B} \int_{T_0}^T k_{tot}(x) dx\right]. \tag{17}$$

This equation (Vass and Demeter 1984; Rappaport et al. 2005) is of course close to Eq. 11, except that we have now two enthalpic parameters, ΔH_{exc} and ΔH_{nr} (in k_{tot}), instead of one. The L expression has the same structure (Eq. 14), i.e., the product of the fraction of the energized state $n(T)$, which decays monotonously, by a gain factor $k_{exc}(T)$, which increases exponentially. At variance with the Randall–Wilkins Eq. 11, the two factors are now uncoupled. For example, it is possible, if $\Delta H_{exc} \gg \Delta H_{nr}$, that the gain factor k_{exc} becomes large only at temperatures where most of the energized state has already decayed. The uncoupling between $k_{exc}(T)$ and $n(T)$ leads to a simple test to discriminate leakage- or deactivation-type TL. In the Randall–Wilkins scheme, the integral of luminescence over time (scanning the full emission range) is a constant, equal to $\Phi n(0)$, the product of the emission yield by the initial amount of the energized state (see Eq. 7). When the emission intensity is expressed as a function of temperature rather than time, the curve is expanded or contracted depending on the warming rate B and one has

$$\int L(T) dT = B \Phi n(0). \tag{18}$$

The property illustrated in Fig. 3A (linear relationship between the integrated TL and the heating rate) is not true any more if some non-radiative pathway is efficient as discussed by Vass and Demeter (1984). The integrated TL will become larger when accelerating the warming ramp because this leaves less time for S_e to decay through the non-radiative

route before the gain factor k_{exc} becomes large. Figure 3B is a plot of the TL integral versus B , showing the data obtained by Cser and Vass (2007) and (blue or black lines) a numerical simulation that takes into account non-radiative recombination. The simulation, based on PS II parameters determined independently (Rappaport et al. 2005), matches the experimental non-linear relationship, confirming the interference of non-radiative recombination.

The transposition of the above treatment based on the scheme of Fig. 1 to the more complex PS II reaction scheme of Fig. 2, introduced in the previous section, is straightforward. There are now four energized states instead of two, and two significant non-radiative recombination pathways (“direct” and “indirect” with subscripts d and i , respectively) instead of one. The involvement of four states seems to require the refinement introduced by DeVault and Govindjee (1990), i.e., taking into account the temperature-dependent spreading of the charge-separated state equilibrating over the four states. However, as noted above, this is not necessary because the energy gap between the lowest of these states ($S_2Q_A^-$) and the other ones is such that it is an excellent approximation ($\sim 10^{-4}$) to assume that this is the only state presenting a significant population during the TL process. Thus, if we retain the notation n for the fraction of the system in the set of charge-separated states, it turns out that n reflects

essentially the population of ($S_2Q_A^-$). In order to take into account the alternative recombination routes one just has to introduce an additional term in k_{tot} , which becomes

$$k_{\text{tot}}(T) = k_i(T) + k_d(T) + k_{\text{exc}}(T) \\ = s_i e^{-\frac{\Delta H_i}{k_B T}} + s_d e^{-\frac{\Delta H_d}{k_B T}} + s_{\text{exc}} e^{-\frac{\Delta H_{\text{exc}}}{k_B T}}. \quad (19)$$

Equation 17 then remains valid with this new expression of k_{tot} inserted.

As pointed out by Rose et al. (2008), however, the DeVault approach should be used when dealing with the recombination of the $S_2Q_B^-$ state (i.e., in the absence of DCMU). In this case, the equilibrium constant between the $S_2Q_A^-$ and $S_2Q_B^-$ states is not large enough (especially in the case of mutants studied by these authors) to neglect the fractional occupancy of the Q_A^- state. Denoting as $K(T)$ the equilibrium constant determining the fraction of centers in which the electron is on Q_A , the fraction of carriers available for recombination is $X(T) = \frac{K(T)}{1+K(T)}$. Equation 17 then becomes

$$L(T) = \Phi s_{\text{exc}} X(T) \exp \left[-\frac{\Delta H_{\text{exc}}}{k_B T} \int_{T_0}^T k_{\text{tot}}(x) X(x) dx \right]. \quad (20)$$

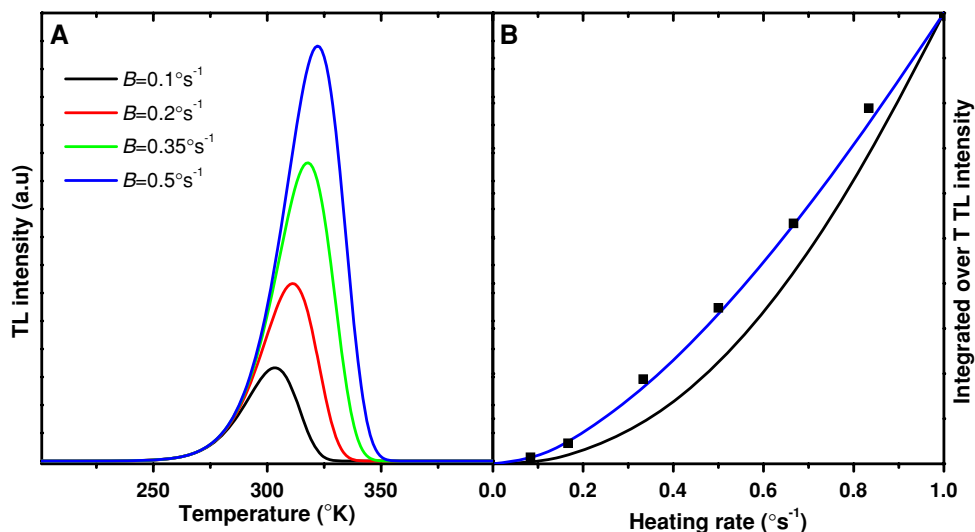


Fig. 3 The effect of the heating rate on the TL intensity. Figure 3A shows the variations in the TL curves associated with changes of the heating rate according to Eq. 11. Figure 3B illustrates the non-linear relationship between TL intensity and the heating rate that results from the presence of a significant non-radiative decay. The data points were replotted from the data of Cser and Vass (2007) for WT PS II. The *black line* is a simulation assuming a monophasic (homogeneous) decay of $S_2Q_A^-$ with a room temperature half-time of 2 s. The *blue line* is a simulation assuming a biphasic decay with the same overall room temperature half-time (see Rappaport et al. 2005).

For the monophasic case, the parameters were: s_{exc} , $1.5 \times 10^9 \text{ s}^{-1}$; ΔH_{exc} , 665 meV; s_i , 10^{10} s^{-1} ; ΔH_i , 630 meV; s_d , 650 s^{-1} ; ΔH_d , 215 meV. In the biphasic case, the parameters of the fast phase (35% relative weight, room temperature half-time of 1 s) were: s_{exc} , $2.2 \times 10^9 \text{ s}^{-1}$; ΔH_{exc} , 665 meV; s_i , $2.2 \times 10^{10} \text{ s}^{-1}$; ΔH_i , 630 meV; s_d , 750 s^{-1} ; ΔH_d , 215 meV. The parameters of the slow component (65% relative weight, room temperature half-time = 6 s) were: s_{exc} , $6 \times 10^8 \text{ s}^{-1}$; ΔH_{exc} , 665 meV; s_i , $6 \times 10^9 \text{ s}^{-1}$; ΔH_i , 630 meV; s_d , 150 s^{-1} , ΔH_d , 215 meV

Photosynthetic TL theory (2): Exciton re-trapping and effect of antenna connectivity

When P* is formed in the luminescence process, there is a significant probability that the excitation is transferred to other chlorophylls, starting an excitonic random walk over the antenna domain. Due to antenna connectivity (several reaction centers share a common light-harvesting antenna), some of these excitons will visit other units before decaying and their fate will depend on the closed/open state of the RC in these units. Therefore, one expects a larger emission yield when (other things being equal) a large fraction of the RCs are in the closed “fluorescent” Q_A⁻ state than when most RCs are in the open “quenching” Q_A state. This should cause some distortion to the TL peak (Ducruet and Miranda 1992) and we would like to examine how this issue can be handled. This is related to the problem discussed in earlier literature of the effect of the fluorescence yield on luminescence (Lavorel 1975; Lavorel et al. 1982).

Clearly, most of the excitons on P* will decay back to a charge-separated state on the same RC, either directly or after some transient trip on neighboring chlorophylls. This local re-trapping, which does not involve the visit of any other RC, is a non-event in our kinetic scheme, because the energized state has not decayed. Therefore, we assume that the rate constants used in the kinetic scheme are duly taking such processes into account. Thus, *k_{exc}* now means the rate constant for net exciton formation (local re-trapping deducted). The excitons, which do escape local re-trapping by the RC, can either decay (through heat or fluorescence) in the local unit (this may be thought as the core antenna close to the RC of origin), with some probability that we denote as *α*, or reach more distant regions with probability 1 - *α*. The following treatment relies on the concepts and notations developed by Lavergne and Trissl (1995). The probability *α* can be estimated as

$$\alpha \approx \frac{k_1}{k_1 + k_{UU}}, \tag{21}$$

where *k₁* is the rate constant for exciton deactivation (through heat or fluorescence) from the antenna in the absence of any quenching by the RCs, and *k_{UU}* is the rate constant for transfer between two units (in a model of “connected units”). With the parameter values advocated in Lavergne and Trissl (1995), one obtains *α* ≈ 0.08. For the (1 - *α*) fraction that leaves the unit of origin, one may assume that the fate of the exciton is basically the same as that of some “average” exciton originating from light absorption. We are then in known ground: for this average exciton, the probability of photochemical trapping by open RCs depends on the fraction *n* of closed RCs in the following way

$$\varphi(n) = \varphi(0) \frac{(1 + J)(1 - n)}{1 + J - Jn}, \tag{22}$$

where *J* is the connectivity parameter (typically ~2.4 in PS II) and *φ*(0) is the photochemical yield when all RCs are open (we adopt *φ*(0) ≈ 0.9 as a reasonable estimate). The “emission yield” *Y*(*n*) from the antenna (lumping light, with a weighting factor of *Φ*, and heat, with that of 1 - *Φ*) is not simply equal to [1 - *φ*(*n*)] because there is some quenching by closed RCs. This accounts for the fact that the ratio *R* = *F_m*/*F₀* between the maximum (*n* = 1) and minimum (*n* = 0) levels of the fluorescence yield is smaller than 1/[1 - *φ*(0)]: for *φ*(0) ≈ 0.9 the latter expression equals 10, while *R* is typically about 5.5. Nevertheless, there is a proportionality relation between the variable parts of the *Y*(*n*) and [1 - *φ*(*n*)] functions, so that

$$Y(n) = 1 - \varphi(0) + (\varphi(0) - \varphi(n)) \frac{(R - 1)(1 - \varphi(0))}{\varphi(0)}. \tag{23}$$

As expected, this expression gives *Y*(0) = 1 - *φ*(0) and *Y*(1) = *R* *Y*(0).

For a given value of *n*, an exciton which escapes its unit of origin has thus three decay routes. It can be trapped by an open RC, which causes no change of *n* (a non-event again). The two other routes, emission from the antenna or quenching by a closed RC, must be taken into account for computing the rate of *n* decay, but only the former will affect the luminescence yield (see below Eq. 26). Thus, the effective decay rate through the excitonic pathway is

$$k_{exc}(\alpha + (1 - \alpha)(1 - \varphi(n))) = k_{exc}(1 - \varphi(n)(1 - \alpha)). \tag{24}$$

The differential equation for *n*(*T*) is now

$$\frac{dn}{dT} = -\frac{1}{B}(k_{exc}(1 - \varphi(n)(1 - \alpha)) + k_r + k_d)n. \tag{25}$$

This cannot be integrated as done previously, because the presence of *φ*(*n*) does not allow variable separation. Numerical integration is required (e.g., using a Runge-Kutta algorithm) to obtain *n*(*T*). When this is done, the TL curve is obtained as

$$L(T) = \Phi n k_{exc}(\alpha + (1 - \alpha)Y(n)). \tag{26}$$

Figure 4 shows the *n*(*T*) curve obtained from the numerical integration of Eq. 25 (red), compared with the treatment ignoring connectivity (blue). Both curves are indistinguishable, which is a consequence of the minor contribution of the excitonic pathway to the overall decay—so that the changes of the re-trapping yield have negligible consequence. As to the TL curves, the effect of connectivity is to enhance the emission when *n* is large, i.e., at low *T*. This results in a small shift of *T_m* to lower temperature (by 2°

with the present parameters). As expected, the two curves become superimposable (not shown) when the simulation is run starting from a small initial n (e.g., using a sub-saturating flash hitting 10% of the RCs): in this case, the relative change of n is too small to affect significantly the yield. One should notice that even when starting from $n = 1$, the distortion caused by antenna connectivity is small because the TL peak occurs in a temperature region where n has already significantly decayed through the non-radiative routes. In reality, the effect illustrated by Fig. 4 will probably be still smaller due to the involvement of slow recombination phases (occurring in a still lower range of n), which is the issue addressed in the next section.

One can apply Eq. 26 to the case of luminescence at fixed T . The modulation by the fluorescence yield is then quite significant, because now $n(t)$ is monitored with a fixed gain k_{exc} . The enhancement factor (comparing the yields for $n \approx 1$ and $n \approx 0$) predicted by Eq. 26 with the parameters introduced above is 3.4 (less than the R value of 5.5, due to the involvement of the local decay probability, α). Thus, according to this treatment, the luminescence induced by a weak flash should have a ~ 3.4 smaller relative intensity (normalized to the fraction of RCs hit by the flash) and slower decay kinetics (~ 2.4 -fold compared with the saturating flash).

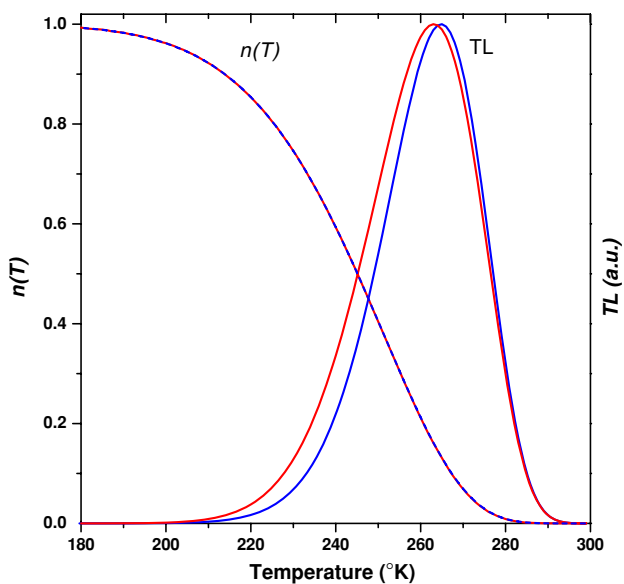


Fig. 4 The effect of antenna connectivity on TL. The $n(T)$ curves were computed using Eq. 25 (taking antenna connectivity into account, *solid red line*) or Eq. 16 (no connectivity, *dotted blue line*). The corresponding TL curves (using Eqs. 17 and 26, respectively) are shown, with normalized amplitudes. The values of the kinetic parameters were the same as in Fig. 3B (homogeneous case), with $B = 0.33 \text{ K s}^{-1}$. A local decay probability $\alpha = 0.08$ and a ratio $R = 5.5$ for F_m/F_0 were assumed

Photosynthetic TL theory (3): Role of kinetic heterogeneity

The kinetic model introduced above still misses a feature of real recombination processes, which happens to have quite significant consequences on TL. As a rule, the recombination reaction in PS II or in purple bacterial RCs is not adequately described as a simple mono-exponential process. For previous literature on this subject, see for PS II: Bennoun (1970); Lavorel et al. (1982); Lavergne and Rappaport (1998); De Wijn et al. (2001); De Wijn and Van Gorkom (2002); and Rappaport et al. (2005) and for bacterial RCs, see Sebban and Wraight (1989); Schoepp et al. (1992); McMahon et al. (1998); Kriegl and Nienhaus (2004). Generally, the recombination kinetics can be fitted satisfactorily as a sum of two exponentials; however, this does not warrant a true bipartite heterogeneity and may very well be due to a more broadly distributed kinetic heterogeneity. Such would be the case if the kinetic complexity stems from the existence of multiple conformation states with different recombination rates. This appears to be the prevailing view both for bacterial RCs (McMahon et al. 1998) and PS II (Lavergne and Rappaport 1998; De Wijn et al. 2001; De Wijn and Van Gorkom 2002; Rappaport et al. 2005).

As noted above, the structure of the TL equation involves the product of a decaying function $n(T)$ representing the amount of energized states by a “gain” term $k_{\text{exc}} = s \exp(-\Delta H_{\text{exc}}/k_B T)$ that increases exponentially with temperature and does so more steeply than the other terms involved in k_{tot} because ΔH_{exc} is the largest enthalpy gap. This means that if some kinetic heterogeneity is present, the slower phases, which appear at higher temperature during the TL ramp, will have the benefit of a higher magnification than the faster phases. If the kinetic heterogeneity stems from a distribution of the enthalpy gaps, one thus expects that the subpopulation with the largest ΔH_i will be over-represented in the TL peak, causing a shift of T_m to high temperatures with respect to the curve that would correspond to the average kinetic parameters of the system.

This effect is illustrated in Fig. 5, where the left-hand side panels in Fig. 5B show simulated TL curves (in black) obtained with the set of parameters derived from kinetics studies in Rappaport et al. (2002) and Cuni et al. (2004), assuming a mono-exponential decay. The right-hand side panels in Fig. 5B show TL curves assuming, more realistically, a heterogeneous population of PS II with 65% of slowly decaying RC as observed in Rappaport et al. (2005). Saliiently, not only is the T_m shifted to higher values but also the TL intensity is much larger, illustrating the enhancement effect introduced above.

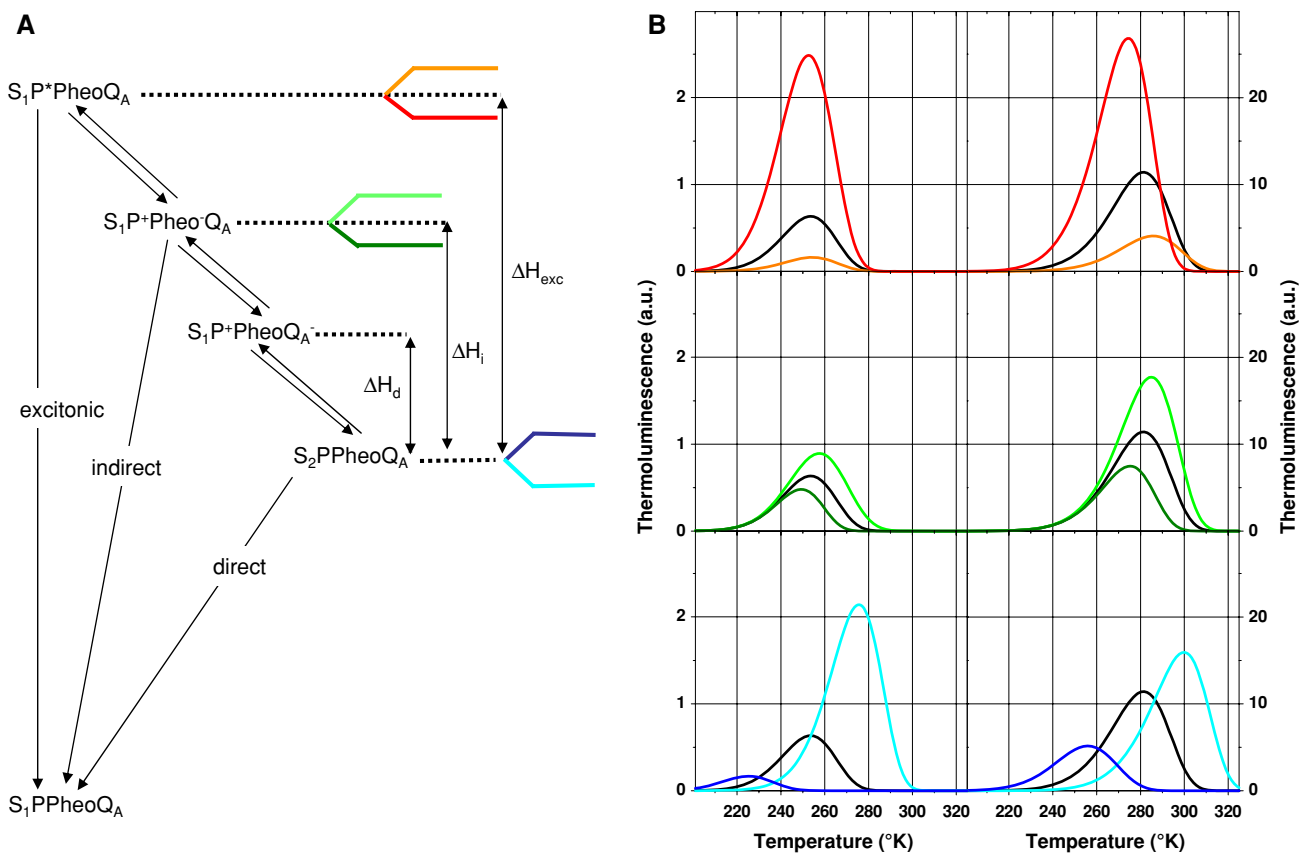


Fig. 5 The consequences of changes in ΔH_{exc} , ΔH_i , or ΔH_d on TL. Figure 5A shows the various changes in energy level considered here with their corresponding color code (each change is ± 30 meV). Figure 5B shows the corresponding TL curves. As in the case of Fig. 3, two different situations are shown. The simulations on the left-

hand side correspond to the homogeneous case and those on the right-hand side to the heterogeneous case. The sets of parameters used here were the same as those used in Fig. 3B. The heating rate is $B = 0.33^\circ\text{C s}^{-1}$

The TL signature in various circumstances

In this section, we give an overview of the theory’s predictions as regards the consequences for TL of changes (e.g., due to mutations) of the energetics of PS II. In Fig. 5A, the scheme is that of Fig. 2, with the color code for changes of the energy levels of three states. The corresponding simulated TL peaks (using Eqs. 17 and 19) are shown in Fig. 5B, assuming a monophasic decay (left-hand plots) or a bi-exponential decay (right-hand plots).

Change of ΔH_{exc}

The top panels of Fig. 5B illustrate the effect of changing the energy level of P* with fixed ΔH_i and ΔH_d . There are no mutations that correspond to a pure change of ΔH_{exc} (i.e., a shift of the absorption spectrum of P₆₈₀, without altering the midpoint potential of the P⁺/P couple), but this case is still of interest as a similar TL signature will result

from an entropic instead of enthalpic change of this energy difference. This is what happens when we change the antenna size: when more antenna chlorophylls are available to excitation transfer, this causes an increase of the entropy (thus a free energy decrease) of P*.

In the range of changes $\Delta\Delta H_{exc}$ explored here (± 30 meV), the radiative recombination pathway remains minor and the $n(T)$ function is little affected. A specific change in ΔH_{exc} alters the equilibrium constant between P* and S₂Q_A⁻ and the gain factor k_{exc} . Thus, when ΔH_{exc} is decreased, the TL intensity is enhanced. The peak temperature, on the other hand, is subjected to opposite effects. The small acceleration of the overall decay due to the increased contribution of k_{exc} in k_{tot} tends to shift the $n(T)$ decay toward lower T , while the steeper dependence of k_{exc} on T tends to shift the TL peak to higher T . Both effects partially cancel out and the result is a very small decrease of T_m when decreasing ΔH_{exc} . The major effect is thus clearly the modulation of the amplitude, which varies as $\exp(-\Delta\Delta G_{exc}/k_B T)$.

Change of ΔH_i

The theoretical effects are illustrated in the middle panels of Fig. 5B. A specific change of ΔH_i leaves the gain factor k_{exc} unchanged, but it affects the $n(T)$ decay function since k_i is the main contributor to k_{tot} in the upper temperature range. With the parameters used here, the direct recombination route is predominant below 250 K, which accounts for the identical TL curves in this region. At higher T , the indirect pathway takes over. Thus, the decay is accelerated when ΔH_i is decreased and both the $n(T)$ function and TL peak are accordingly shifted toward lower T . The effect on the amplitude is then purely due to the gain factor k_{exc} that enhances the TL emission all the more as it occurs at higher T .

This case has been experimentally investigated with PS II mutants from *Synechocystis* sp. 6803 bearing site-directed replacements of the D₁-Gln130 residue (Giorgi et al. 1996) that is involved in a H-bond with the C₁₃=O of Pheo_A (Moënne-Loccoz et al. 1989). Varying the strength of the H-bond modifies the redox potential of the Pheo/Pheo[−] couple (the stronger the H-bond the more positive the redox potential). The resulting increase (decrease) in ΔH_i was associated with an increased (decreased) TL intensity. In addition, the changes in intensity were correlated to changes in the same direction of the T_m (Rappaport et al. 2005; Cser and Vass 2007); an unexplained exception is the Q130L mutant in the presence of DCMU which showed an increased intensity with no changes in T_m (Cser and Vass 2007).

Another case of mutants in which ΔH_i is modified is the site-directed mutants of D₁-His198, a residue which provides an axial ligand to one of the two Chls of P (Diner et al. 2001). These mutations, however, are more ambiguous than those of D₁-Gln130 since the shift in the midpoint potential of the P⁺/P couple not only affects the energy level of the P⁺Pheo[−] state (and thus ΔH_i) but also that of the P⁺Q_A[−] state (and thus ΔH_d). In addition, the D₁-His198Gln mutation induces a blue-shift of the absorption bands of P (Diner et al. 2001) and thus modifies the energy level of the P* state as well (and thus ΔH_{exc}). Despite their “pleiotropic” consequences on the energetic landscape of PS II, the TL phenotype of these mutations is in line with our expectations. Indeed, an up-shift of the midpoint potential of the P⁺/P couple and thus increased ΔH_i and ΔH_d resulted in an enhanced TL and, conversely, a down-shift was associated with a decreased TL. Cser and Vass (2007) proposed that the changes of the TL intensity in both the D₁-Gln130 and D₁-His198 mutants depend essentially on the free energy gap between P* and P⁺Pheo[−], varying as $\exp(\Delta(\Delta G_{\text{exc}} - \Delta G_i)/k_B T)$, where T is taken close to the T_m of the wild type (WT). When direct recombination can be neglected, this energy gap controls

Table 1 Estimates of the free energy changes (in meV) associated with the D₁-Gln130 or D₁-His198 mutations derived from: (a) fast transient absorption of the P⁺Pheo[−] radical pair measured 60 ps after the exciting pulse (Merry et al. 1998); (b) changes in the midpoint potential of the P⁺/P couple estimated from charge recombination kinetics (Diner et al. 2001); (c) TL studies assuming that the ratio between the intensities of the TL curves is $\exp((\Delta G_{\text{exc}} - \Delta G_i)/k_B T)$ (Cser and Vass 2007)

	$\Delta G(\text{P}^+\text{Pheo}^-)$ (a)	$\Delta G(\text{P}^+\text{Q}_A^-)$ (b)	$\Delta G_{\text{exc}} - \Delta G_i$ (c)
Q130L	74		52
Q130E	−33		−38
H198 K		88	80
H198A		−70	−30
H198Q		0-50	23

the relative weight of recombination through the radiative and non-radiative routes and, thus, the TL intensity. As shown in Table 1, this approximate relation is in satisfactory agreement with the available data.

Change of the lowest energy level

This is the case illustrated by the lower panels in Fig. 5B. In practice, this may arise from changes affecting the S-states, e.g., by substitution of Ca²⁺ or Cl[−] for Sr²⁺ or Br[−], respectively (Ishida et al. 2008). Under the same heading, one may also place TL comparisons between the states S₂Q_A[−] (DCMU present) and S₂Q_B[−] or S₃Q_B[−] (no inhibitor) as well as PS II mutants affecting the midpoint potential of the Q_A/Q_A[−] or Q_B/Q_B[−] couples (see Mäenpää et al. 1995; Fufezan et al. 2007; Rose et al. 2008).

A change of the lowest energy level affects similarly ΔH_d , ΔH_i , and ΔH_{exc} ; thus, all contributions to k_{tot} are modified in the same direction, with little change in the relative weights of each decay pathway. This results in a shift of the $n(T)$ decay function and TL band to higher or lower T when the energy level of S₂Q_A[−] is lowered or raised, respectively. An amplitude effect accompanies these temperature shifts: as usual, the higher the T_m , the larger the enhancement; but the effect is smaller than in the preceding case, because one has now a correlation between a higher T_m and a lower k_{exc} . The signature of such changes is thus a significant change in T_m and a moderate one in the TL intensity.

The numerical simulations indicate that, with the set of parameters used here, T_m depends steeply and almost linearly on ΔH_d with a slope of $\sim 0.4^\circ \text{ meV}^{-1}$. This dependence may provide estimates of the free energy changes associated with TL modifications. As an example, the T_m of the S₂Q_B[−] TL band is up-shifted by ~ 12 K with respect to that of the S₂Q_A[−] band (Vass et al. 1981; Rutherford et al. 1984a, b). Based on the numerical simulations shown here, this locates S₂Q_B[−] about 30 meV below S₂Q_A[−] in the

presence of DCMU. Since in the presence of DCMU the energy level of $S_2Q_A^-$ is down-shifted by about 50 mV (Krieger et al. 1995), the free energy change associated with the electron transfer between Q_A^- and Q_B^- would be ~ 80 meV, in agreement with the value derived from kinetic study (Diner 1977; Lavergne 1982). As another example, Rose et al. (2008) recently characterized various PS II site-directed mutants in the Q_B pocket. These mutants displayed a T_m down-shifted by ~ 10 K, and applying a similar formalism as the one described here, Rose et al. concluded that this shift reflects an up-shifted midpoint potential for the Q_B/Q_B^- couple by ~ 30 mV.

For a discussion of methods used in Thermoluminescence, see Ducruet and Vass (this issue).

Acknowledgment We thank Govindjee for editing this paper.

References

- Arnold W, Sherwood HK (1957) Are chloroplasts semiconductors? Proc Natl Acad Sci USA 43:105–114. doi:10.1073/pnas.43.1.105
- Barter LMC, Klug DR, Van Grondelle R (2005) Energy trapping and equilibration: a balance of regulation and efficiency. In: Wydrzynski TJ, Satoh K (eds) Photosystem II: the light driven water: plastoquinone oxidoreductase. Advances in Photosynthesis and Respiration, vol 22. Springer, Dordrecht, pp 491–514
- Bennoun P (1970) Reoxidation of the fluorescence quencher “Q” in the presence of 3-(3, 4-dichlorophenyl)-1,1-dimethylurea. Biochim Biophys Acta 216:357–363. doi:10.1016/0005-2728(70)90227-6
- Booth PJ, Crystall B, Ahmad I, Barber J, Porter G, Klug DR (1991) Observation of multiple radical pair states in photosystem 2 reaction centers. Biochemistry 30:7573–7586. doi:10.1021/bi00244a029
- Borisov AY, Godik VI, Kotova EA, Samuilov VD (1980) Membrane potential effect on nanosecond recombination luminescence in *Rhodospirillum rubrum*. FEBS Lett 119:121–124. doi:10.1016/0014-5793(80)81012-X
- Cser K, Vass I (2007) Radiative and non-radiative charge recombination pathways in Photosystem II studied by thermoluminescence and chlorophyll fluorescence in the cyanobacterium *Synechocystis* 6803. Biochim Biophys Acta 1767:233–243. doi:10.1016/j.bbabi.2007.01.022
- Cuni A, Xiong L, Sayre RT, Rappaport F, Lavergne J (2004) Modification of the pheophytin midpoint potential in Photosystem II: modulation of the quantum yield of charge separation and of charge recombination pathways. Phys Chem Chem Phys 6:4825–4831. doi:10.1039/b407511k
- De Grooth BG, Van Gorkom HJ (1981) External electric field effects on prompt and delayed fluorescence in chloroplasts. Biochim Biophys Acta 635:445–456. doi:10.1016/0005-2728(81)90104-3
- De Wijn R, Van Gorkom HJ (2002) The rate of charge recombination in Photosystem II. Biochim Biophys Acta 1553:302–308. doi:10.1016/S0005-2728(02)00183-4
- De Wijn R, Schrama T, Van Gorkom HJ (2001) Secondary stabilization reactions and proton-coupled electron transport in photosystem II investigated by electroluminescence and fluorescence spectroscopy. Biochemistry 40:5821–5834. doi:10.1021/bi002824z
- DeVault D, Govindjee (1990) Photosynthetic glow peaks and their relationship with the free energy change. Photosynth Res 24: 175–181
- DeVault D, Govindjee, Arnold W (1983) Energetics of photosynthetic glow peaks. Proc Natl Acad Sci USA 80:983–987. doi:10.1073/pnas.80.4.983
- Diner BA (1977) Dependence of the deactivation reactions of photosystem II on the redox state of plastoquinone pool varied under anaerobic conditions Equilibria on the acceptor side of photosystem II. Biochim Biophys Acta 460:247–258. doi:10.1016/0005-2728(77)90211-0
- Diner BA, Britt RD (2005) Tyrosines YZ and YD in Photosystem II. In: Wydrzynski TJ, Satoh K (eds) Photosystem II: the light driven water: plastoquinone oxidoreductase. Advances in Photosynthesis and Respiration, vol 22. Springer, Dordrecht, pp 207–233
- Diner BA, Schlodder E, Nixon PJ, Coleman WJ, Rappaport F, Lavergne J, Vermaas WF, Chisholm DA (2001) Site-directed mutations at D1-His198 and D2-His197 of photosystem II in *Synechocystis* PCC 6803: sites of primary charge separation and cation and triplet stabilization. Biochemistry 40:9265–9281. doi:10.1021/bi010121r
- Ducruet J-M, Miranda T (1992) Graphical and numerical analysis of thermoluminescence and fluorescence F_0 emission in photosynthetic material. Photosynth Res 33:15–27. doi:10.1007/BF00032979
- Ducruet J-M, Vass I (2009) Thermoluminescence: experimental. Photosynth Res (this issue). doi:10.1007/s11120-009-9436-0
- Fufezan C, Gross CM, Sjodin M, Rutherford AW, Krieger-Liszak A, Kirilovsky D (2007) Influence of the redox potential of the primary quinone electron acceptor on photoinhibition in photosystem II. J Biol Chem 282:12492–12502. doi:10.1074/jbc.M610951200
- Giorgi LB, Nixon PJ, Merry SAP, Joseph DM, Durrant JR, Rivas JD, Barber J, Porter G, Klug DR (1996) Comparison of primary charge separation in the photosystem II reaction center complex isolated from wild-type and D1-130 mutants of the cyanobacterium *Synechocystis* PCC 6803. J Biol Chem 271:2093–2101. doi:10.1074/jbc.271.4.2093
- Grabolle M, Dau H (2005) Energetics of primary and secondary electron transfer in Photosystem II membrane particles of spinach revisited on basis of recombination-fluorescence measurements. Biochim Biophys Acta 1708:209–218. doi:10.1016/j.bbabi.2005.03.007
- Hillier W, Messenger J (2005) Mechanism of photosynthetic oxygen production. In: Wydrzynski TJ, Satoh K (eds) Photosystem II: the light-driven water: plastoquinone oxidoreductase. Advances in Photosynthesis and Respiration, vol 22. Springer, Dordrecht, pp 567–608
- Inoue Y, Shibata K (1979) Thermoluminescence from the oxygen-evolving system in photosynthesis. Trends Biochem Sci 4:182–184. doi:10.1016/0968-0004(79)90420-1
- Ishida N, Sugiura M, Rappaport F, Lai TL, Rutherford AW, Boussac A (2008) Biosynthetic exchange of bromide for chloride and strontium for calcium in the photosystem II oxygen-evolving enzymes. J Biol Chem 283:13330–13340. doi:10.1074/jbc.M710583200
- Joliot P, Joliot A, Bouges B, Barbieri G (1971) Studies of system II photocenters by comparative measurements of luminescence, fluorescence, and oxygen emission. Photochem Photobiol 14: 287–305. doi:10.1111/j.1751-1097.1971.tb06174.x
- Krieger A, Rutherford AW, Johnson GN (1995) On the determination of redox midpoint potential of the primary quinone electron acceptor, Q_A , in photosystem II. Biochim Biophys Acta 1229:193–201. doi:10.1016/0005-2728(95)00002-Z

- Kriegl JM, Nienhaus GU (2004) Structural, dynamic, and energetic aspects of long-range electron transfer in photosynthetic reaction centers. *Proc Natl Acad Sci USA* 101:123–128. doi:10.1073/pnas.2434740100
- Lavergne J (1982) Mode of action of 3-(3, 4-dichlorophenyl)-1,1-dimethylurea. Evidence that the inhibitor competes with plastoquinone for binding to a common site on the acceptor side of photosystem II. *Biochim Biophys Acta* 682:345–353. doi:10.1016/0005-2728(82)90048-2
- Lavergne J, Rappaport F (1998) Stabilization of charge separation and photochemical misses in photosystem II. *Biochemistry* 37:7899–7906. doi:10.1021/bi9801210
- Lavergne J, Trissl H-W (1995) Theory of fluorescence induction in Photosystem II: derivation of analytical expressions in a model including exciton-radical pair equilibrium and restricted energy transfer between photosynthetic units. *Biophys J* 65:2474–2492. doi:10.1016/S0006-3495(95)80429-7
- Lavorel J (1975) Luminescence. In: Govindjee (ed) *Bioenergetics of photosynthesis*. Academic Press, San Francisco, pp 223–317
- Lavorel J, Lavergne J, Etienne A-L (1982) A reflection on several problems of luminescence in photosynthetic systems. *Photobiophys* 3:287–314
- Mäenpää P, Miranda T, Tyystjarvi E, Tyystjarvi T, Govindjee, Ducruet JM, Etienne AL, Kirilovsky D (1995) A mutation in the D-de loop of D-1 modifies the stability of the $S_2Q_A^-$ and $S_2Q_B^-$ states in photosystem II. *Plant Physiol* 107:187–197
- McMahon BH, Muller JD, Wraight CA, Nienhaus GU (1998) Electron transfer and protein dynamics in the photosynthetic reaction center. *Biophys J* 74:2567–2587. doi:10.1016/S0006-3495(98)77964-0
- Merry SAP, Nixon PJ, Barter LMC, Schilstra MJ, Porter G, Barber J, Durrant JR, Klug D (1998) Modulation of quantum yield of primary radical pair formation in photosystem II by site directed mutagenesis affecting radical cations and anions. *Biochemistry* 37:17439–17447. doi:10.1021/bi980502d
- Miallier D, Sanzelle S, Pilleyre T, Bassinet C (2006) Residual thermoluminescence for sun-bleached quartz: dependence on pre-exposure radiation dose. *Quat Geochronol* 1:313–319
- Moëne-Loccoz P, Robert B, Lutz M (1989) A resonance Raman characterization of the primary electron acceptor in Photosystem II. *Biochemistry* 28:3641–3645. doi:10.1021/bi00435a003
- Peloquin JM, Williams JC, Lin XM, Alden RG, Taguchi AKW, Allen JP, Woodbury NW (1994) Time-dependent thermodynamics during early electron transfer in reaction centers from *Rhodospirillum rubrum*. *Biochemistry* 33:8089–8100. doi:10.1021/bi00192a014
- Randall JF, Wilkins JHF (1945) Phosphorescence and electron traps. The study of trap distributions. *Proc R Soc Lond A* 184:366–389
- Rappaport F, Diner BA (2008) Primary photochemistry and energetics leading to the oxidation of the Mn_4Ca cluster and to the evolution of molecular oxygen in Photosystem II. *Coord Chem Rev* 252:259–272. doi:10.1016/j.ccr.2007.07.016
- Rappaport F, Guergova-Kuras M, Nixon PJ, Diner BA, Lavergne J (2002) Kinetics and pathways of charge recombination in photosystem II. *Biochemistry* 41:8518–8527. doi:10.1021/bi025725p
- Rappaport F, Cuni A, Xiong L, Sayre R, Lavergne J (2005) Charge recombination and thermoluminescence in photosystem II. *Biophys J* 88:1948–1958. doi:10.1529/biophysj.104.050237
- Renger G, Holzwarth AR (2005) Primary electron transfer in Photosystem II. In: Wydrzynski TJ, Satoh K (eds) *Photosystem II: the light-driven water: plastoquinone oxidoreductase*. *Advances in Photosynthesis and Respiration*, vol 22. Springer, Dordrecht, pp 139–175
- Rose S, Minagawa J, Seufferheld M, Padden S, Svensson B, Kolling DR, Crofts AR, Govindjee (2008) D1-arginine257 mutants (R257E, K, and Q) of *Chlamydomonas reinhardtii* have a lowered QB redox potential: analysis of thermoluminescence and fluorescence measurements. *Photosynth Res* 98:449–468. doi:10.1007/s11120-008-9351-9
- Rutherford AW, Govindjee, Inoue Y (1984a) Charge accumulation and photochemistry in leaves studied by thermoluminescence and delayed light emission. *Proc Natl Acad Sci USA* 81:1107–1111. doi:10.1073/pnas.81.4.1107
- Rutherford AW, Renger G, Koike H, Inoue Y (1984b) Thermoluminescence as a probe of photosystem II. The redox and protonation states of the secondary acceptor quinone and the oxygen-evolving enzyme. *Biochim Biophys Acta* 767:548–556. doi:10.1016/0005-2728(84)90054-9
- Sane PV, Rutherford AW (1986) Thermoluminescence from photosynthetic membranes. In: Govindjee, Ames J, Fork DC (eds) *Light emission by plants and bacteria*. Academic Press, New York, pp 329–362
- Schoepp B, Parot P, Lavorel J, Verméglio A (1992) Charges recombination kinetics in bacterial photosynthetic reaction centers: conformational states in equilibrium pre-exist in the dark. In: Breton J, Verméglio A (eds) *The photosynthetic reaction center II*. Plenum Press, New York, pp 331–339
- Sebban P, Wraight CA (1989) Heterogeneity of the $P^+Q_A^-$ recombination kinetics in reaction centers from *Rhodospirillum rubrum*: the effect of pH and temperature. *Biochim Biophys Acta* 974:54–65. doi:10.1016/S0005-2728(89)80165-3
- Van Gorkom HJ (1985) Electron transfer in Photosystem II. *Photosynth Res* 6:97–112. doi:10.1007/BF00032785
- Vass I, Demeter S (1984) Energetic characterization of the thermoluminescence in isolated chloroplast. In: Sybesma C (ed) *Advances in photosynthesis research*, vol 1. Martinus Nijhoff/Dr. W. Junk publishers, The Hague, Netherlands, pp 737–740
- Vass I, Govindjee (1996) Thermoluminescence of the photosynthetic apparatus. *Photosynth Res* 48:117–126. doi:10.1007/BF00041002
- Vass I, Horvath G, Herczeg T, Demeter S (1981) Photosynthetic energy conservation investigated by thermoluminescence, activation energies and half-lives of thermoluminescence bands determined by mathematical resolution of glow curves. *Biochim Biophys Acta* 634:140–152. doi:10.1016/0005-2728(81)90134-1
- Vavilin DV, Vermaas WF (2000) Mutations in the CD-loop region of the D2 protein in *Synechocystis* sp. PCC 6803 modify charge recombination pathways in photosystem II in vivo. *Biochemistry* 39:14831–14838. doi:10.1021/bi001679m